PCCP

Accepted Manuscript

ROYAL SOCIETY OF CHEMISTRY

www.rsc.org/pccp

Physical Chemistry Chemical Physics
CREATED USING THE RSC LaTeX PCCP ARTICLE TEMPLATE – SEE www.rsc.org/electronicfiles FOR DETAILS
ARTICLE TYPE www. rsc.org/x XXXXXXXX

The importance of polarizability: Comparison of models of carbon disulphide in the ionic liquids $[C_1C_1im][NTf_2]$ and $[C_4C_1im][NTf_2]$

Ruth M.Lynden-Bell,[*a] **and Edward L. Quitevis,**[b]

Received Xth XXXXXXXXXX 20XX, Accepted Xth XXXXXXXXX 20XX
First published on the web Xth XXXXXXXXXX 200X
DOI: 10.1039/b000000x

The local environment of CS_2 and in solution in two ionic liquids ($[C_1C_1im][NTf_2]$ and $[C_4C_1im][NTf_2]$) are investigated by atomistic simulation and compared with that in neat CS_2. The intermolecular vibrational densities of states of CS_2 are calculated and compared with experimental OHD-RIKES spectra. The fair agreement of the results from solutions but poor agreement of the results from neat CS_2 suggest that while collective effects are unimportant in solutions, they have a major effect on the OHD-RIKES spectrum of neat CS_2. Comparing polarizable and unpolarizable models for CS_2 emphasizes the importance of polarizability in determining local structure.

1 Introduction

The solvation mechanism of molecular solutes in ionic liquids (ILs) can be quite different than in conventional molecular solvents not only because of the ionicity of ILs[1] but also because of their nanoscale structural heterogeneity. That such heterogeneity is present in ILs was first evidenced by molecular dynamics (MD) simulations of ILs based on 1-alkyl-3-methylimidazolium ($[C_nC_1im]^+$)[2–4] and experimentally by small-wide X-ray scattering (SWAXS) measurements on $[C_nC_1im][Cl]$ and $[C_nC_1im][BF_4]$.[5] Initially, the existence of heterogeneity in ILs was met with scepticism, particularly in the assignment of the prepeak in the total scattering function S(q) to nanoscale correlations associated with this heterogeneity.[6] However, these doubts have largely been laid to rest by Margulis and coworkers[7] who through the use of MD simulations showed how S(q) can be resolved into components corresponding to correlations between the types of charge-density regions reflecting this heterogeneity.

The heterogeneity in ILs is characterized by nonpolar domains (low-charge density regions) embedded or intertwined with polar domains (high-charge density regions) that arise from the nanosegregation of the alkyl tails, with the degree of structural heterogeneity being dictated by the length of the C_n-alkyl tails. Recent MD simulations on the $[C_nC_1im][NTf_2]$ series of ILs, where $[NTf_2]^-$ is the bis[(trifluoromethane)sulfonyl]amide anion, reveal a more complex picture of the evolution of the morphology with increasing alkyl chain length from isolated 'hydrocarbon-like islands in the midst of a continuous polar network' for short chains (n = 2- 4) that percolate to form a continuous nonpolar microphase for longer alkyl chains with the percolation threshold occurring at n = 6.[8] Given this scenario of polar and nonpolar domains, the modes of solvation of molecular solutes can be understood from the chemical adage 'like dissolves like' with nonpolar solutes residing in the low-charge density regions, polar protic solutes in the high-charge density regions, and polar aprotic solutes at the interface between the high-charge and low-charge density regions, as shown, respectively, in simulations of mixtures of hexane/$[C_6C_1im][PF_6]$, H_2O/$[C_6C_1im][PF_6]$, and CH_3CN/$[C_6C_1im][PF_6]$.[9,10] Recent experimental measurements of butane and isobutane in imidazolium-based ILs backed by MD simulations, provide further support for nonpolar aprotic alkane solutes being localized in the low-charge density regions of the IL.[11,12] Nonpolar aromatic solutes, such as benzene, are a special case because of their propensity to interact with the imidazolium ring through local electrostatic interactions giving rise to π-stacking.[13–17]

In a recent study, Xue et al.[18] found that mixtures of certain nonpolar aprotic solutes and $[C_1C_1im][NTf_2]$ appear to be at odds with the paradigm of nonpolar solutes residing mainly in the low-charge density regions. Because $[C_1C_1im][NTf_2]$ lacks the long C_n chain (n > 2) required to form nonpolar domains, the solubility of a nonpolar aprotic solute must solely be determined by its interaction with the high-charge density part of $[C_1C_1im][NTf_2]$. They found that upon mixing, a 10 mol% mixture of CCl_4 and $[C_1C_1im][NTf_2]$ formed an optically clear solution, whereas a 10 mol% mixture of n-pentane and $[C_1C_1im][NTf_2]$ formed a cloudy emulsion. Similar results were obtained for the 20 mol% mixtures of CCl_4 and $[C_1C_1im][NTf_2]$ and n-pentane and $[C_1C_1im][NTf_2]$. In contrast, a 10 mol% mixture of CS_2 and $[C_1C_1im][NTf_2]$ formed an optically clear solution, whereas a 20 mol% mix-

[a] *Department of Chemistry, University of Cambridge, Cambridge CB2 1EW, UK. E-mail: rmlb@cam.ac.uk*
[b] *Department of Chemistry and Biochemistry, Texas Tech University, Lubbock, TX 79409, USA. edward.quitevis@ttu.edu*

ture of CS_2 and $[C_1C_1im][NTf_2]$ formed a cloudy emulsion. These tests showed the relative solubilities in $[C_1C_1im][NTf_2]$ at room temperature to be in the order n-pentane $<$ CS_2 $<$ CCl_4. As CS_2 is polarizable it can interact with the high-charge density regions of the IL via charge-induced dipole forces. Therefore, the greater the molecular polarizability of the solute, the greater is its solubility in $[C_1C_1im][NTf_2]$. Given that the mean molecular polarizability of CCl_4 (11.7×10^{-40} J $V^{-2}m^2$)[19] is greater than that of CS_2 (9.7×10^{-40} J $V^{-2}m^2$),[19] this correlation between polarizability and solubility is consistent with solubility of CCl_4 in $[C_1C_1im][NTf_2]$ being greater than that of CS_2. Because the molecular polarizability of n-pentane (11.1×10^{-40}J V^{-2} m^2)[19] is almost equal to that of CCl_4, one would have predicted that the solubilities of n-pentane and CCl_4 should be the same, and that n-pentane should have a greater solubility than CS_2, which is contrary to the results of the solubility tests. Because solvation in the high-charge density regions of the IL involves disruption of the charge-order, the size of the solute must also be considered in that small solutes would be more readily accommodated in the charge-ordered network than large solutes. This would explain the relative observed solubilities of CCl_4 and n-pentane, even though they have nearly the same polarizabilities. As the molecular volume of n-pentane (V_{vdW} = 107 Å^3) is larger than CCl_4 (V_{vdW} = 88.3 Å^3)) and CS_2 (V_{vdW} = 55.6 Å^3)), we would predict that the solubility of n-pentane to be less than that of CS_2 and CCl_4, in agreement with the solubility tests. However, using solute size alone, we would also predict that the solubility of CS_2 should be greater than that of CCl_4, contrary to the solubility tests. Therefore, in the solvation of nonpolar, nonaromatic solutes in $[C_1C_1im][NTf_2]$, the polarizability of a solute appears to play a greater role than its molecular size.

CS_2 is often used as a reference in OHD-RIKES spectroscopy as its large anisotropic polarizability gives a strong signal.[20–24] Xue et al.[18] have made measurements of the Kerr spectra of solutions of CS_2 in $[C_nC_1im][NTf_2]$. In order to model these systems in computer simulations one needs a model for the interaction of CS_2 with the other species present.

We wondered whether it was important to include the polarizability of CS_2 in the simulation or whether properties of the mixture would be described adequately by a non-polarizable model. To investigate this we have compared simulations of CS_2 in $[C_1C_1im][NTf_2]$ and $[C_4C_1im][NTf_2]$ using different models of CS_2. We find that while the properties of solutions of CS_2 in the ionic liquid are much the same for models with and without charges, including polarizability affects the local structure considerably. We find considerable differences between the imidazolium ionic liquid with a butyl side chain and one with a methyl side chain which we attribute to the presence and absence of non-polar domains in the liquid. Of course the S atoms of CS_2 are not the only polarizable atoms in the system, but with the computational resources available to us it is not practical to make all the atoms polarizable. Kerr spectra of solutions of solutions of CS_2[18,20–24] show that the dominant contribution comes from the anisotropically polarizable CS_2. Hence in this current work we only include the polarizability of CS_2.

2 Models and simulation conditions.

CS_2 has been modelled in computer simulations for many years. Tildesley and Madden[25] first introduced a model with three Lennard-Jones sites on a rigid CS_2 molecule which gave good liquid properties. This is our first model, the T&M model. However the molecule has a quadrupole moment[26] and our second model, the charged model, has charged sites in addition to the Lennard-Jones terms. The charges are taken from Torii[27] which were chosen to fit the electrostatic field around a molecule. Although Torii showed that one needs site quadrupoles in addition to site charges to obtain a good fit to the electrostatic field of the molecule, we have not included such terms. Our third model includes polarizability - the polarizable model. Polarizability was modelled using the shell model with shells on the two sulphur sites, but with no interactions between sites in the same molecule. This model does not account for the difference in molecular polarizability parallel and perpendicular to the symmetry axis, but does allow the molecule to respond to an unsymmetric environment. The polarisability of CS_2 has been measured[28,29] and calculated[30] to be approximately 14Å^3 parallel and 5.5Å^3 perpendicular to the molecular axis. The force constant for the harmonic core-shell interaction was chosen to give an atomic polarizability volume, α_S of 7Å^3 by setting it to 2431 kJ/Å^2. The mass of each shell was set equal to 0.5 amu with a corresponding reduction of the mass of the core. The charge of each sulfur atom is divided to give a charge of -3.5e on the shell and +3.618e on the core. Additional runs with a model with half the polarizability were carried out, the halfpol model. Again no intramolecular polarization was allowed. Simulations of neat CS_2 showed that the Lennard-Jones σ parameters had to be increased in the polarizable model to obtain a pressure near 1 atmosphere. The values used for the C and S potential parameters are shown in Table 1.

The models for the $[C_1C_1im]^+$ and $[C_4C_1im]^+$ were taken from the work of Canongia Lopes and Padua[31] while that for $[NTf_2]^-$ was taken from Köddermann et al.[32]. Note that while the cation potential is an all-atom potential, the anion potential is a 9-site potential with united CF_3 groups. In all cases the Lennard-Jones cross terms were calculated using Lorentz-Berthelot combining rules.[33]

Molecular dynamics simulations were performed with a modified version of the program DL_POLY[34] using the dynamic shell model. Runs were performed with time steps of 2fs for the unpolarized models and 0.5fs for the polariz-

able models. Several independent runs were carried out in the NVT ensemble at 300K with a Nose Hoover thermostat with time constant=0.5ps. The electrostatics was calculated using an Ewald sum with precision 10^{-5}. This corresponds to the Ewald parameters $\alpha = 2.2470 \times 10^{-1}$Å^{-1} and a maximum k vector equal to (8 8 8). The stability of the Ewald sum was checked by monitoring the Coulomb energy and Coulomb virial, which remained constant and equal and opposite within the required precision. The real space cutoff for both the Ewald and the Lennard-Jones terms was chosen to be 1.25nm. Some runs were made at 400K where the molecular structure equilibrates more rapidly to check that the systems were equilibrated. The periodically repeated cubic cell with dimensions 37.0Å^3 contained 124 ion pairs and 8 CS_2 molecules, that is a molar percentage of 6%. Note the maximum solubility recently measured in our laboratory is 13%.

Table 1 Potential parameters for C and S sites in CS_2 in the four models. The values for the Lennard-Jones ε_{ii} are in kJ/mol, for σ_{ii} are in nm and the polarizability volume α_S is in Å^3.

	ε_{CC}	σ_{CC}	q_C/e	ε_{SS}	σ_{SS}	α_S
T&M	0.4257	0.335	0.	1.521	0.352	0.
charged	0.4257	0.335	-0.236	1.521	0.352	0.
polarizable	0.4257	0.33853	-0.236	1.521	0.3552	7.0
halfpol	0.4257	0.33853	-0.236	1.521	0.3552	3.6

3 Energetics

We can compare the energetics of the interaction of a CS_2 molecule with the two ionic liquids for the different models. This shows both the effects of including polarizability and the difference due to the side chain.

The data in Table 2 show that the Lennard-Jones energy of CS_2 in $[C_1C_1im][NTf_2]$ is almost the same for all the models. This term dominates the energy in the charged model and the half polarizable model, and even in the fully polarizable model it is comparable to the electrostatic energy. One must also include the cost of polarizing the molecules in the total energy, which is given in the table. The errors were calculated from the variation between different runs. It is noteworthy that the electrostatic interactions are much more negative and the polarization energies are higher in solutions in either of these ionic liquids than in a simulation of a pure liquid of the fully polarizable model of CS_2. In the neat liquid the net electrostatic energy (Coulomb plus polarization) is only -0.7kJ/mol in contrast to -24.3kJ/mol in the ionic liquid environment. Increasing the temperature of $[C_1C_1im][NTf_2]$ from 300K to 400K results in the total interaction energies becoming less negative by about 2kJ/mol.

There is an interesting difference between the $[C_1C_1im]^+$ and $[C_4C_1im]^+$ cations. While the Lennard-Jones energy in the $[C_4C_1im][NTf_2]$ ionic liquid is more negative by about 4kJ/mol than in the $[C_1C_1im][NTf_2]$ liquid, the electrostatic energy of the polarizable model in $[C_4C_1im][NTf_2]$ is about half the value as it is in $[C_1C_1im][NTf_2]$. This is the result of changes in the local environment of the CS_2 molecule. In $[C_4C_1im][NTf_2]$ the CS_2 has a high probability of being in the non-polar domains near the cation tails rather than near the charged domains near the rings. In $[C_1C_1im][NTf_2]$, however, the cation side chains are too short to form non-polar domains and the CS_2 interacts more strongly with the charged ring.

Table 2 Contributions[(a)] to the interaction energy of CS_2 with surroundings (in kJ/mol per CS_2 molecule)

	T&M	charged	halfpol	polarizable
	$[C_1C_1im][NTf_2]$			
ES	0	-2.32 ± 0.1	-11.0 ± 0.3	-52.6 ± 2.0
LJ	-35.2 ± 0.2	-35.7 ± 0.2	-36.2 ± 0.2	-34.7 ± 0.2
Epol	0	0	$+3.9 \pm 0.1$	$+23.8 \pm 0.8$
total	-35.2 ± 0.2	-38.0 ± 0.2	-43.3 ± 0.4	-63 ± 2
	$[C_4C_1im][NTf_2]$			
ES		-1.82 ± 0.03		-23.4 ± 0.6
LJ		-37.6 ± 0.2		-39.2 ± 0.1
Epol		0		$+14.9 \pm 0.4$
total		-39.5 ± 0.2		-47.6 ± 0.2
	CS_2 (neat)			
ES	0	-0.11		$-1.97 \pm .01$
LJ	-24.5	-24.5		$-25.1 \pm .01$
Epol	0	0		$1.24 \pm .01$
total	-24.5	-24.6		$-25.8 \pm .01$

[(a)] ES:Coulomb; LJ:Lennard-Jones; Epol: energy of polarization

4 Local environment

4.1 Radial distribution functions

Radial distribution functions were calculated for a number of cation and anion sites relative to C and S sites on the CS_2 molecules. These show rather little change for anion sites, but a dramatic change for cation sites.

Figure 1 shows radial distribution functions between the ring carbon atoms in both $[C_1C_1im]^+$ and $[C_4C_1im]^+$ and the centre of the CS_2 molecule for various models. In $[C_1C_1im][NTf_2]$ there is a big change in the radial distribution function for C_2, the unique carbon atom on the $[C_1C_1im]^+$ ring. As polarization is added the CS_2 molecule is attracted to this atom and its probability density becomes more localised. The distributions relative to the adjacent carbon atoms in the ring, C_4 and C_5, also show a similar, but less pronounced, effect. On the other hand in $[C_4C_1im][NTf_2]$ there is much less change on adding polarisability. This can be attributed to the attraction of the CS_2 molecules to the butyl side chain. Figure

2 demonstrates that the distance of closest approach of CS_2 to the anion is longer than to the cation. The various models give essentially the same radial distributions relative to the central N site of $[NTf_2]$ (=$[N(SO_2CF_3)_2]^-$) and rather small changes to the peripheral O sites.

Figure 3 is interesting because it shows that in the charged model there is a strong tendency for the CS_2 molecules to be near the tail, especially near to the terminal methyl group. On the other hand the tendency is less marked for the polarizable CS_2 molecules.

The radial distribution functions from the CS_2 molecule to the central site (N) and the O sites on the anions show that the CS_2 molecules do not approach the anions as closely as the cations; the first peak is at 5Å for O and 7Å for N. There is little difference between the models. In summary, CS_2 molecules tend to be closer to the cations than to the anions particularly in the polarizable model. The distributions are also more structured in the latter.

Values for the number of nearest neighbours for the central C of CS_2 can be calculated from these radial distribution functions. There are on average about 0.6 cations in the sharp first peak of the polarizable model (to 4.1Å), which is considerably larger than for the other models. Including the second peak one obtains about 3.3 neighbours, which is the same as the number to this distance for the other models. This shows that, in this model, some cations from the first shell of neighbours are pulled close to the CS_2 molecule.

4.2 Spatial distribution functions

More insight into these changes can be found by looking at the spatial probability distribution functions for CS_2 around the cations. In Figures 4 and 5 these functions are shown for the charged models and the polarizable models of $[C_1C_1im][NTf_2]$ and $[C_4C_1im][NTf_2]$. First, comparing the polarizable and unpolarizable models, we see that in both liquids the distributions around the cations are much more localised in the polarizable models (red) than in the charged models (blue). Note that in both liquids the density contours used to show the distributions are 3 times the average for the polarizable models but only 1.3 times the average for the charged models. If the higher cutoff were used for the charged models nothing would be seen. There are considerable differences in the distributions around the two cations. For $[C_1C_1im]^+$ polarizable CS_2 tends to lie above and below the unique CH bond, while near $[C_4C_1im]^+$ polarizable CS_2 tends to lie above and below the ring. The charged CS_2 models have a broad band of high probability around $[C_4C_1im]^+$, but the regions of high probability for this model lie to the back of the $[C_1C_1im]^+$ cation near the adjacent C atoms.

Finally in Figure 6 we see the distributions from the point of view of a CS_2 molecule. This figure shows concentrations of $[C_1C_1im]^+$ cations (above) and $[NTf_2]^-$ anions (below) in a plane containing a polarizable CS_2 molecule. The cation positions are defined by the central point of the NN vector, while the anions are described by the positions of the four oxygen atoms. We see that the greatest concentration of cations is near the central C atom, while the anions tend to be near the S atoms where they also interact with the cations around the central C atom. The localisation is much less marked in the unpolarizable models (not shown).

Table 3 First moments (M_1) and maximum frequencies (ν_{max}) of density of states[(a)] for polarizable CS_2 in ionic liquid solutions and in neat CS_2. Values in cm^{-1}.

	$[C_4C_1im][NTf_2]$		$[C_1C_1im][NTf_2]$		CS_2 (neat)	
	M_1	ν_{max}	M_1	ν_{max}	M_1	ν_{max}
CS_2 lib	56.1	40	67	45(b)	52	30(b)
CS_2 trans	49.3	28(b)	57	26(b)	47	13
OKE	35	21	36	24	44	28

[(a)] (b) denotes a broad band.

5 Comparison of Densities of States

Figure 7 shows the intermolecular part of the CS_2 vibrational density of states in different environments. In the neat liquid both the translational and vibrational contributions are broader and have a lower frequency than in ionic liquid solutions. There is rather little difference between the two ionic liquid solvents, but in $[C_4C_1im][NTf_2]$ the response is slightly sharper with a higher maximum than in $[C_1C_1im][NTf_2]$; note that as the area under these graphs is constant the width and height are inversely correlated. In both ionic liquids the maxima in the librational and translational densities of states are blue-shifted relative to the neat liquid.

5.1 Comparison of calculated densities of states with OKE spectra

In the study in which the solubility tests were done, Xue et al.[18] also measured the Kerr spectra of 10 mol% CS_2/$[C_nC_1im][NTf_2]$ mixtures for n = 1-4 using optical heterodyne-detected Raman-induced Kerr effect spectroscopy (OHD-RIKES). The Kerr spectra of these mixtures were fitted by the sum of a CS_2 component and an IL component, which was taken to be equal to the Kerr spectra of the neat IL. They found that the CS_2 component was lower in frequency and narrower than the Kerr spectrum of neat CS_2, in agreement with an earlier OHD-RIKES study of CS_2/$[C_5C_1im][NTf_2]$ mixtures.[35–37] For the purposes of the comparison with densities of states calculated in the current simulation study, the CS_2 contributions to the Kerr spectra of 10 mol% mixtures of CS_2

in $[C_1C_1im][NTf_2]$ and $[C_4C_1im][NTf_2]$ and the Kerr spectrum of neat CS_2 at 295 K are show in Figure 8. Values of the spectral maxima, ν_{max}, and the first spectral moments, M_1, for both simulations and observations are listed in Table 3.

As we explained in a recent article,[16] densities of states by their very nature, cannot be directly compared to Kerr spectra, because densities of states are calculated from single particle velocity correlation functions (VCF), whereas Kerr spectra arise from the fluctuations in the collective polarizability anisotropy. From the perspective of instantaneous normal mode (INM) analysis one can go from a density of states to a Kerr spectrum by weighting each of modes in the density of states by the square of the derivative of the total polarizability anisotropy with respect to the canonical coordinates associated with the modes.[38] In principle using a dipole-induced dipole model Kerr spectra can also be simulated.[39–43] However due to the time, RAM, and disk storage required to calculate collective polarizabilities, the simulation of Kerr spectra for ILs is challenging.[44] In contrast densities of states are less difficult to calculate than Kerr spectra. Indeed, in a recent study of 1:1 benzene/$[C_1C_1im][NTf_2]$ mixture, the densities of states were found to be consistent with the intermolecular Kerr spectra. In the current study of CS_2/$[C_1C_1im][NTf_2]$ and CS_2/$[C_4C_1im][NTf_2]$ mixtures the densities of states are only partly consistent with the intermolecular Kerr spectra.

Table 3 shows values of the first moments, M_1, of the densities of states for polarizable CS_2 dissolved in $[C_4C_1im][NTf_2]$, in $[C_1C_1im][NTf_2]$, and in neat liquid calculated from the simulations together with values of M_1 obtained from OHD-RIKES measurements shown in Fig.8. For simulations the values of M_1 are given for the translational and librational contributions (M_1(trans) and M_1(lib)). The first moment M_1 being an average over the entire spectrum provides a means of quantifying the differences between spectra with broad asymmetric line-shapes such as those obtained in simulations or OHD-RIKES measurements. From the spectral moments in Table 3, we see that the total, librational, and translational moments are higher in frequency for CS_2 in $[C_1C_1im][NTf_2]$ (M_1^{MD}(lib) = 67 cm^{-1}, M_1^{MD}(trans) = 57 cm^{-1}) than for CS_2 $[C_4C_1im][NTf_2]$ (M_1^{MD}(lib) = 56 cm^{-1}, M_1^{MD}(trans) = 49 cm^{-1}). A similar pattern is observed for values of the spectral maxima. This difference is consistent with the OHD-RIKES measurements where the intermolecular spectrum is higher in frequency for CS_2 in $[C_1C_1im][NTf_2]$ (M_1^{OKE} = 36 cm^{-1}) than for CS_2 in $[C_4C_1im][NTf_2]$ (M_1^{OKE} = 35 cm^{-1}). However, this difference is small and within the 1 cm^{-1} experimental uncertainty of the measurements. But Figure 8 clearly shows the intermolecular spectrum to be higher in frequency for CS_2 in $[C_1C_1im][NTf_2]$ than for CS_2 in $[C_4C_1im][NTf_2]$. Because the intermolecular spectra of CS_2 in these ionic liquids are characterized by single bands with well-defined lineshapes, the spectral maxima are better indicators of the frequencies of the Kerr spectra than the first spectral moments. Indeed, based on the spectral maxima, the intermolecular spectrum of CS_2 is slightly higher in frequency in $[C_1C_1im][NTf_2]$ (ν_{max} = 24 cm^{-1}) than in $[C_4C_1im][NTf_2]$ (ν_{max} = 21 cm^{-1}). Interestingly, we find that based on the first spectral moments, the librational and translational densities of states of neat CS_2 are lower in frequency than those of either CS_2 in $[C_1C_1im][NTf_2]$ or CS_2 in $[C_4C_1im][NTf_2]$, which is inconsistent with the results of the OHD-RIKES measurements, where M_1^{OKE} = 44 cm^{-1} for neat CS_2 versus M_1^{OKE} = 35 cm^{-1} for CS_2 in $[C_4C_1im][NTf_2]$ and M_1^{OKE} = 36 cm^{-1} for CS_2 in $[C_1C_1im][NTf_2]$. This discrepancy, which at first glance seems surprising, can be rationalised by remembering that a density of states is a reflection of single particle dynamics, whereas the Kerr spectrum is related to the dynamics of the collective polarizability anisotropy . Thus the difference may yield further insight into the molecular interactions in mixtures of CS_2 and ILs. In the initial OHD-RIKES study of mixtures of CS_2 and $[C_5C_1im][NTf_2]$ by Xiao et al.,[35] the idea that at low concentrations CS_2 molecules are isolated from each other and are localized in the nonpolar domains of the IL was based on the CS_2 contribution to the Kerr spectrum of a 5 mol% mixture of CS_2 and $[C_5C_1im][NTf_2]$ being similar to the Kerr spectrum of a 5 mol% mixture of CS_2 in n-pentane, with the spectrum being lower in frequency and narrower than that of neat CS_2. Subsequent MD simulations of this mixture system confirmed that CS_2 molecules are isolated from each other and mainly localized in the nonpolar domains.[36] A red-shift and line narrowing are commonly observed in OKE spectra upon dilution of weakly interacting systems, such as CS_2 in alkane mixtures.[22,23,45–47] Thus we attribute the higher frequency in the OKE spectrum of the neat liquid compared with the ionic liquid solutions to increased collective interactions between CS_2 molecules in the neat liquid.

The underlying mechanism for these effects is, however, controversial.[47] In one mechanism the spectral changes are attributed to the softening of the effective intermolecular potential seen by CS_2 molecules upon dilution.[24,48] In another mechanism, the spectral changes are attributed to a decrease in interaction-induced effects upon dilution.[46] In the previous studies of CS_2/IL mixtures,[18,35–37] the spectral changes were primarily attributed to softening of the intermolecular potential. However, the current studies suggest that these modes are not softened (see Table 3) and that the decrease in the interaction induced effects must be playing an important role in the observed spectral changes observed in CS_2/IL mixtures compared with the neat liquid. For liquids comprised of anisotropic molecules, the collective polarizability anisotropy TCF can be resolved into a molecular autocorrelation, an interaction-induced (I-I) correlation, and molecular-induced cross correlation.[49–51] The molecular term relaxes through single-molecule reorientation, whereas the induced

terms (autocorrelation and cross correlation) relax through intermolecular motions. If there is a difference in the time scales of reorientational and intermolecular motions, which is the case for CS_2,[50,51] the induced part of the polarizability that follows reorientation can be projected out. The result is that the TCF can then be re-expressed as the sum of a local-field modified molecular reorientation term, a collision-induced term, and a collision-induced cross correlation, with the collision-induced terms contributing to the high-frequency part of the spectrum. Without invoking softening of the intermolecular potential, one could easily explain the red-shift and line-narrowing of the Kerr spectra as being due to the decrease in the contribution of the high-frequency collision-induced terms upon dilution in going from the CS_2 molecules in the neat liquid to CS_2 molecules isolated from each other in the CS_2/$[C_1C_1im][NTf_2]$ and CS_2/$[C_4C_1im][NTf_2]$ mixtures. That the density of states of CS_2 in the neat liquid is lower in frequency than that the densities of states of CS_2 in the CS_2/$[C_1C_1im][NTf_2]$ and CS_2/$[C_4C_1im][NTf_2]$ mixtures is not inconsistent with this explanation because the densities of states being single particle properties cannot account for collision-induced effects and in some respects would only correspond to the molecular reorientational part of the time correlation function of polarizability anisotropy. The data in Table 2 indicate that the interaction energy is greater for CS_2 in the ionic liquids than in the neat liquid. This would explain why the density of states is higher in frequency for CS_2 in the ionic liquids than in the neat liquid. If we assume that the molecular reorientational part of the polarizability anisotropy TCF behaves in the same way as the densities of states, then red-shift and line-narrowing of the Kerr spectrum of CS_2 in going from the neat liquid to the mixtures cannot be due the softening of the intermolecular potential seen by the CS_2 but is due to purely a dilution effect that results in the diminished role of the collision-induced terms of the polarizability anisotropy TCF.

6 Previous simulations

Prior to this study, MD simulations were performed on 5, 10, and 20% mixtures of CS_2 and $[C_5C_1im][NTf_2]$ and on neat CS_2 and $[C_5C_1im][NTf_2]$.[36] As in the current study, the previous simulations were done in order to understand the Kerr spectra of these solutions. Briefly, the total potential energy in these simulations was described by the Amber force field with the parameters for the $[C_5C_1im]^+$ cation provided by the standard Amber force field and the parameters for the $[NTf_2]^-$ anion from the work of Lopes and Pádua.[52] For CS_2 a non-polarizable rigid-body model was used that included van der Waals and Coulombic interactions with parameters from the Amber force field. The model used in this previous study is therefore analogous to the charged model in the current study. In the previous study the system sizes were approximately half those in the current study. For example, for the 5% mixture, which is comparable to the 6% mixtures in the current study, the system was comprised of 72 ion pairs and four CS_2 molecules. This previous study also differs from the current study in that only radial distribution functions for various sites on $[C_5C_1im]^+$ and $[NTf_2]^-$ relative to the C site on CS_2 were calculated. Although these previous simulations were not performed with exactly the same force field as the current simulations, the results are similar with regards to the location of CS_2 in the ionic liquid as reflected in the radial distribution functions. The radial distribution functions in both simulations of CS_2 in $[C_4C_1im][NTf_2]$ and CS_2 in $[C_5C_1im][NTf_2]$ thus show CS_2 molecules being closer to the terminal groups of the cation alkyl tails than to imidazolium ring or the anions, which is consistent with CS_2 being mainly localized in the non-polar domains of the ionic liquids.

7 Conclusions

In order to model solutions of CS_2 in imidazolium ionic liquids we find that it is necessary to include the polarizability of CS_2; this affects both the local structure and the energetics of solvation in the highly polar environment of the ionic liquids $[C_1C_1im][NTf_2]$ and $[C_4C_1im][NTf_2]$. The presence of a non-polar side chain in $[C_4C_1im]^+$ reduces the concentration of CS_2 molecules near the cation ring and increases it near the tails. However this trend is less marked when polarizability is included and electrostatic interactions increase in importance. The spectra of the densities of states of CS_2 in the ionic liquids are shifted to higher frequencies than in the neat liquid, which is consistent with the increased interaction energy. In contrast, the frequency of Kerr spectrum of CS_2 is lower in frequency in ionic liquid solutions than in the neat liquid. Previously, this spectral shift was attributed to a softening of the intermolecular potential. However, the simulation results for the density of states shows that the intermolecular potential of a single CS_2 is harder in ionic liquid solutions than in neat liquid so that the spectral shift observed in the OKE spectrum is probably a manifestation of the diminished role of interaction-induced terms in the polarizability anisotropy time correlation function that occurs upon dilution in the ionic liquid.

Acknowledgements

Support to ELQ was provided by the National Science Foundation under Grant CHE 1153077 for the research described in this paper.

References

1 J. E. W. Castner, J. F. Wishart and H. Shirota, *Acc. Chem. Res.*, 2007, **40**, 1217–1227.
2 S. M. Urahata and M. C. C. Ribeiro, *J. Chem. Phys.*, 2004, **120**, 1855–1863.
3 Y. Wang and G. A. Voth, *J. Am. Chem. Soc.*, 2005, **127**, 12192–12193.
4 J. N. A. C. Lopes and A. A. H. Pádua, *J. Phys. Chem. B*, 2006, **110**, 3330–3335.
5 A. Triolo, O. Russina, H.-J. Bleif and E. D. Cola, *J. Phys. Chem. B*, 2007, **111**, 4641–4644.
6 C. Hardacre, J. D. Holbrey, C. L. Mullan, T. G. A. Youngs and D. T. Bowron, *J. Chem. Phys.*, 2010, **133**, 074510.
7 H. K. Kashyap, J. J. Hettige, H. V. R. Annapureddy and C. J. Margulis, *Chem. Commun.*, 2012, **48**, 5103–5105.
8 K. Shimizu, M. F. C. Gomes, A. A. H. Pádua, L. P. N. Rebelo and J. N. A. C. Lopes, *J. Mol Struc-THEOCHEM*, 2010, **946**, 70–76.
9 J. N. A. C. Lopes, M. F. C. Gomes and A. A. H. Pádua, *J. Phys. Chem. B*, 2006, **110**, 16816–16818.
10 A. A. H. Pádua, M. F. C. Gomes and J. N. A. C. Lopes, *Acc. Chem. Res.*, 2007, **40**, 1087–1096.
11 M. F. C. Gomes, L. Pison, A. S. Pensado and A. A. H. Pádua, *Faraday Discuss.*, 2012, **154**, 41–52.
12 L. Pison, K. Shimizu, G. Tama, J. N. A. C. Lopes, E. L. Quitevis and M. F. C. Gomes, *Phys. Chem. Chem. Phys.*, 2015, **17**, 30328–30342.
13 M. Deetlefs, C. Hardacre, M. Nieuwenhuyzen, O. Sheppard and A. K. Soper, *J. Phys. Chem. B*, 2005, **109**, 1593–1598.
14 C. G. Hanke, A. Johansson, J. B. Harper and R. M. Lynden-Bell, *Chem. Phys. Lett.*, 2003, **374**, 85–90.
15 J. B. Harper and R. M. Lynden-Bell, *Mol. Phys.*, 2004, **102**, 85–94.
16 R. M. Lynden-Bell, L. Xue, G. Tamas and E. L. Quitevis, *J. Chem. Phys.*, 2014, **141**, 044506.
17 L. Xue, G. Tamas, R. P. Matthews, A. J. Stone, P. A. Hunt, E. L. Quitevis and R. M. Lynden-Bell, *Phys. Chem. Chem. Phys.*, 2015, **17**, 9973–9983.
18 L. Xue, G. Tamas, E. Gurung and E. L. Quitevis, *J. Chem. Phys.*, 2014, **140**, 164512.
19 K. J. Miller, *J. Am. Chem. Soc.*, 1990, **112**, 8533–8542.
20 B. I. Greene and R. C. Farrow, *Chem. Phys. Lett.*, 1983, **98**, 273–275.
21 C. Kalpouzos, W. T. Lotshaw, D. McMorrow and G. A. Kenney-Wallace, *J. Phys. Chem.*, 1987, **91**, 2028–2030.
22 C. Kalpouzos, D. McMorrow, W. T. Lotshaw and G. A. Kenney-Wallace, *Chem. Phys. Lett.*, 1988, **150**, 138–146.
23 C. Kalpouzos, D. McMorrow, W. T. Lotshaw and G. A. Kenney-Wallace, *Chem. Phys. Lett.*, 1989, **155**, 240–242.
24 A. Scodinu and J. T. Fourkas, *J. Phys. Chem. B*, 2003, **107**, 44–51.
25 D. Tildesley and P. Madden, *Mol. Phys.*, 1981, **42**, 1137.
26 M. Battaglia, A. D. Buckingham, D. Neumark, R. K. Pierens and J. H. Williams, *Mol. Phys.*, 1981, **43**, 1015–1020.
27 H. Torii, *J. Chem. Phys.*, 2003, **119**, 2192–2198.
28 G. R. Alms, A. K. Burnham and W.H.Flygare, *J. Chem. Phys.*, 1975, **63**, 3321 –3326.
29 M. P. Bogaard, A. D. Buckingham, R. K. Pierens and A. H. White, *J. Chem. Soc.- Farad.Trans. 1*, 1978, **74**, 3008–3015.
30 G. Maroulis, *Chem. Phys. Letts.*, 1992, **199**, 250–256.
31 J. Canongia Lopes and A. Pádua, *Theoretical Chemistry Accounts*, 2012, **131**, 1129.
32 T. Kodderman, D. Paschek and R. Ludwig, *ChemPhysChem*, 2007, **8**, 2464.
33 M. Allen and D. Tildesley, *Computer Simulation of Liquids;*, Oxford University Press, 2nd edn, 1991.
34 W. Smith, T. Forester and I. Todorov, *The DL POLY Classic User Manual*, STFC Daresbury Laboratory, 2012.
35 D. Xiao, L. . G. Hines, S. Li, R. Bartsch and E. Quitevis, *J. Phys. Chem. B*, 2009, **113**, 4544–4548.
36 P. Yang, G. A. Voth, D. Xiao, L. Hines, R. A. Bartsch and E. L. Quitevis, *J. Chem. Phys.*, 2011, **135**, 034502.
37 E. L. Quitevis, F. Bardak, D. Xiao, L. G. Hines, P. Son, R. A. Bartsch, P. Yang and G. A. Voth, Ionic Liquids: Science and Applications, 2012, pp. 271–287.
38 R. L. Murry, J. T. Fourkas and T. Keyes, *J. Chem. Phys.*, 1998, **109**, 2814–2825.
39 S. Ryu and R. M. Stratt, *J. Phys. Chem. B*, 2004, **108**, 6782–6795.
40 B. M. Ladanyi and Y. Q. Liang, *J. Chem. Phys.*, 1995, **103**, 6325–6332.
41 G. Tao and R. M. Stratt, *J. Phys. Chem. B*, 2006, **110**, 976–987.
42 M. D. Elola, B. M. Ladanyi, A. Scodinu, B. J. Loughnane and J. T. Fourkas, *J. Phys. Chem. B*, 2005, **109**, 24085–24099.
43 M. D. Elola and B. M. Ladanyi, *J. Phys. Chem. B*, 2006, **110**, 15525–15541.
44 Z. Huand, X. Huang, H. V. R. Annapureddy and C. J. Margulis, *J. Phys. Chem. B*, 2008, **112**, 7837–7849.
45 D. McMorrow, N. Thantu, J. S. Melinger, S. K. Kim and W. T. Lotshaw, *J. Phys. Chem.*, 1996, **100**, 10389–10399.
46 T. Steffen, N. A. C. M. Meinders and K. Duppen, *J. Phys. Chem. A*, 1998, **102**, 4213–4221.
47 D. McMorrow, N. Thantu, V. Kleinman, J. S. Melinger and W. T. Lotshaw, *J. Phys. Chem. A*, 2001, **105**, 7960–7972.
48 Q. Zhong and J. T. Fourkas, *J. Phys. Chem. B*, 2008, **112**, 15529–15539.
49 T. Keyes, D. Kivelson and J. P. McTague, *J. Chem. Phys.*, 1971, **55**, 4096.
50 P. A. Madden and D. J. Tildesley, *Mol. Phys.*, 1985, **55**, 969–998.
51 T. I. Cox, M. R. Battaglia and P. A. Madden, *Mol. Phys.*, 1979, **38**, 1539–1554.
52 J. N. A. C. Lopes and A. A. H. Pádua, *J. Phys. Chem. B*, 2004, **108**, 16893–16898.

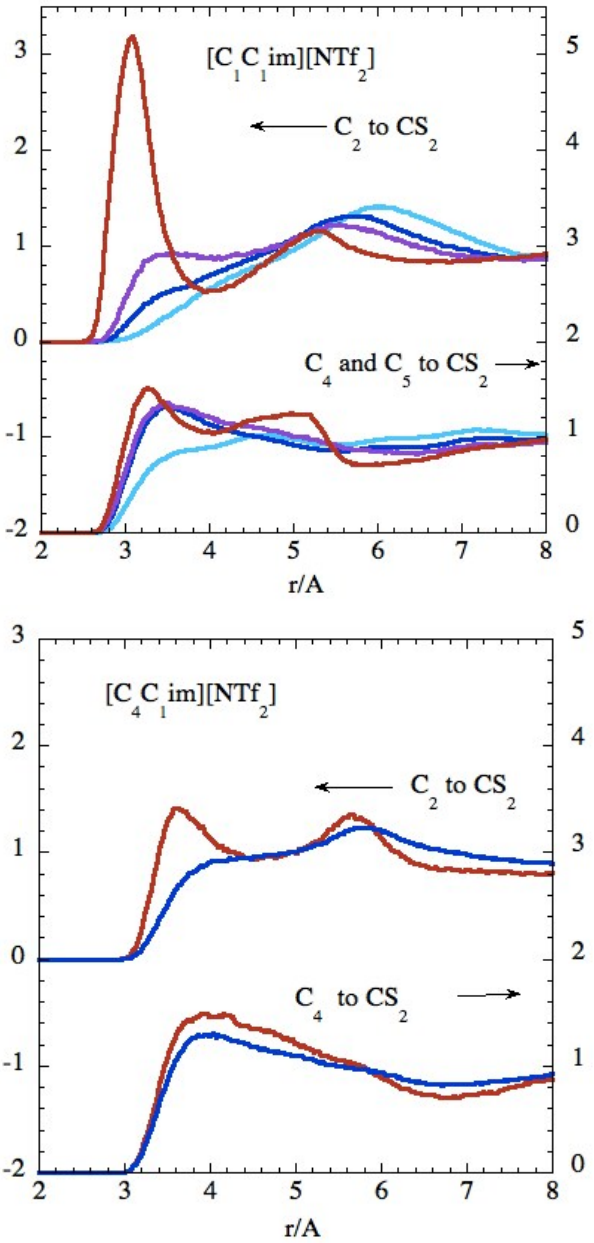

Fig. 1 Effect of polarizability on g(r) between CS_2 and cation ring sites, C_2, C_4 and C_5. Above: $[C_1C_1im][NTf_2]$ showing Tildesley-Madden model (cyan), charged model (blue), half-polarizable model (purple) and polarizable model (red). Below: $[C_4C_1im][NTf_2]$ for the charged model (blue) and the polarizable model (red).

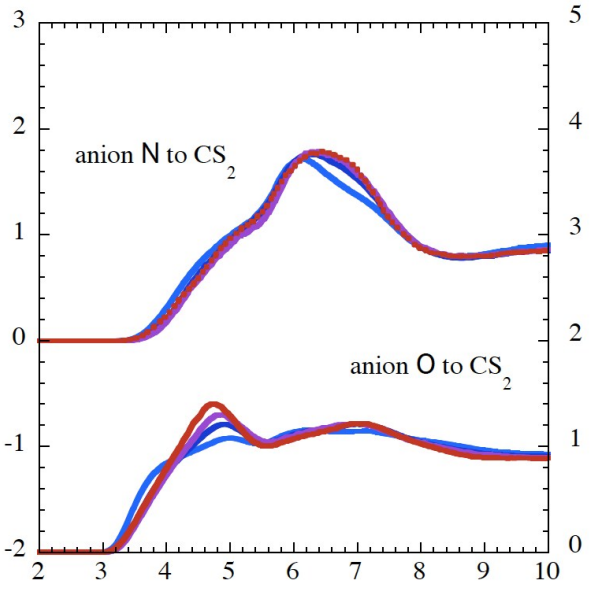

Fig. 2 Effect of polarizability on g(r) between CS_2 and anion sites, N and O, in $[C_1C_1im][NTf_2]$ solution. Above: N site showing Tildesley-Madden model (blue), charged model (cyan), half-polarizable model (purple) and polarizable model (red).

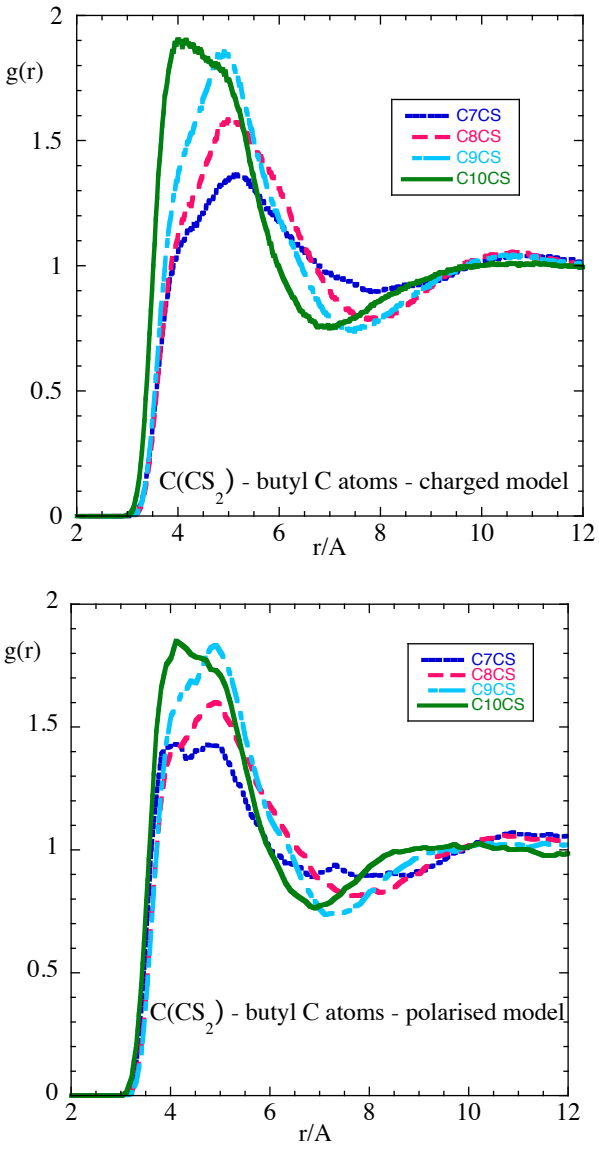

Fig. 3 Radial distribution function between the centre of CS_2 and the 4 carbon atoms in the butyl side chain. C7 is attached to the imidazolium ring and C10 is the terminal carbon atom. Above:charged model; below: polarizable model. Note the preference for the tail group (C10) is decreased when polarizability is included.

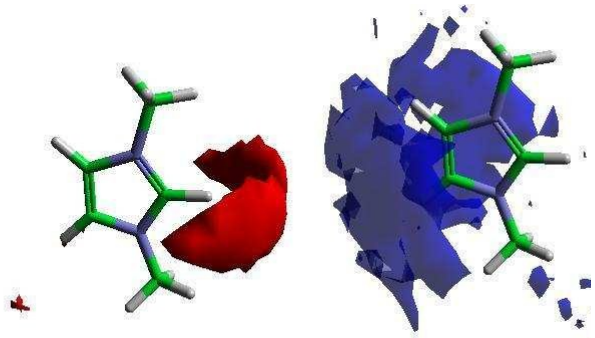

Fig. 4 Three dimensional distribution of CS_2 around a $[C_1C_1im]^+$ ion. Red: polarizable model, cutoff 2.5 times average number density; blue: charged unpolarizable model, cutoff 1.3 times average number density.

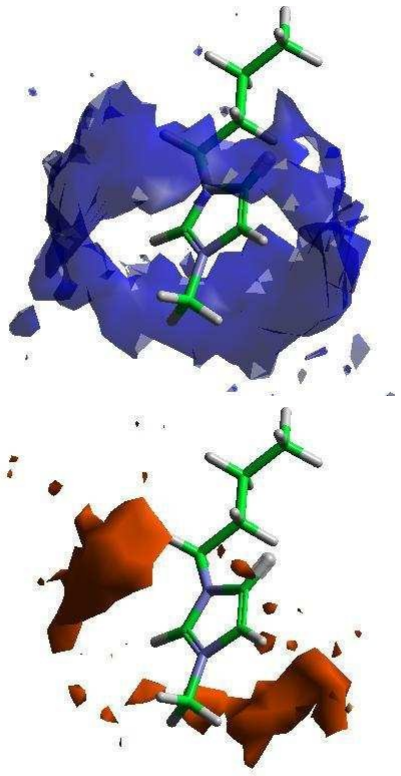

Fig. 5 Three dimensional distribution of CS_2 around a $[C_4C_1im]^+$ ion. Red: polarizable model, cutoff 3 times average number density; blue: charged unpolarizable model, cutoff 1.3 times average number density.

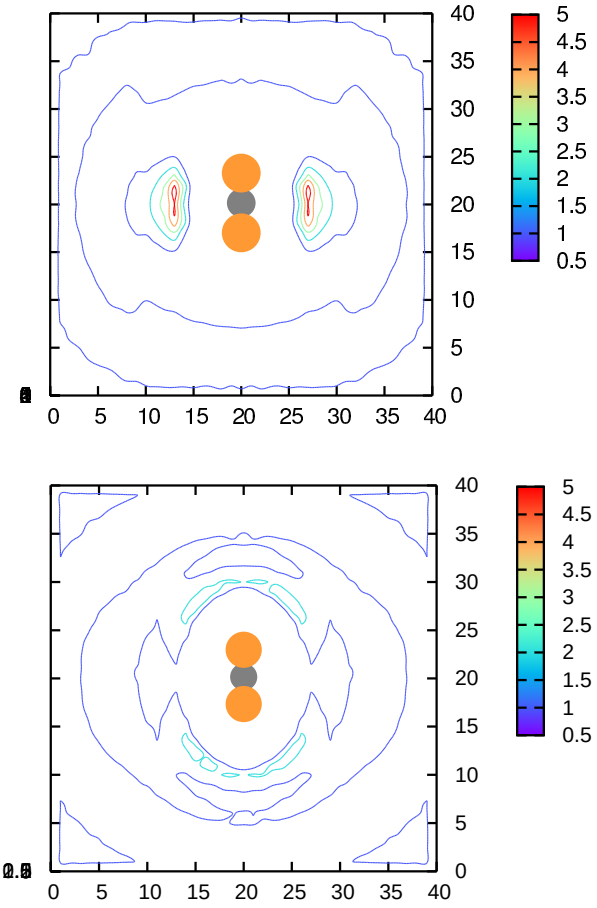

Fig. 6 Cross sections of 3d distributions of ionic liquid ions around a polarizable CS_2 molecule in $[C_1C_1im][NTf_2]$. The contour scale is the number density relative to the bulk value. The x and y scales are in units of 0.5Å. Above: concentration of ring centres; below: concentration of anion oxygen atoms.

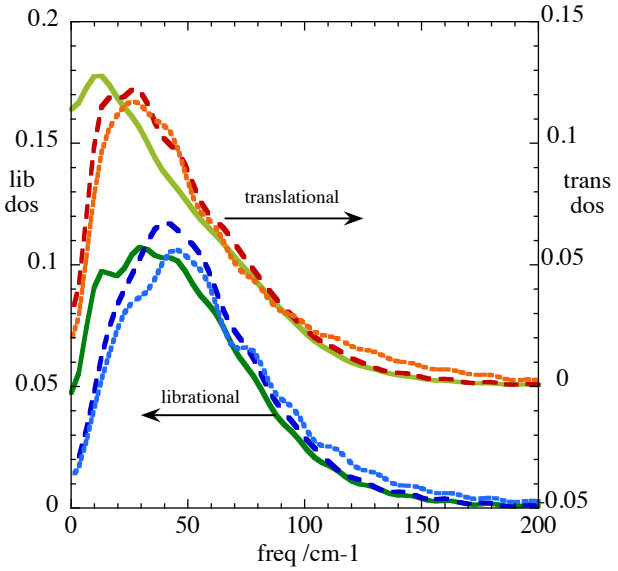

Fig. 7 Vibrational densities of states for polarisable CS_2 in three environments. Solid lines: neat CS_2; dashed lines CS_2 in $[C_4C_1im][NTf_2]$; dotted lines CS_2 in $[C_1C_1im][NTf_2]$. The translational contributions are displaced by 1 unit relative to the librational contributions.

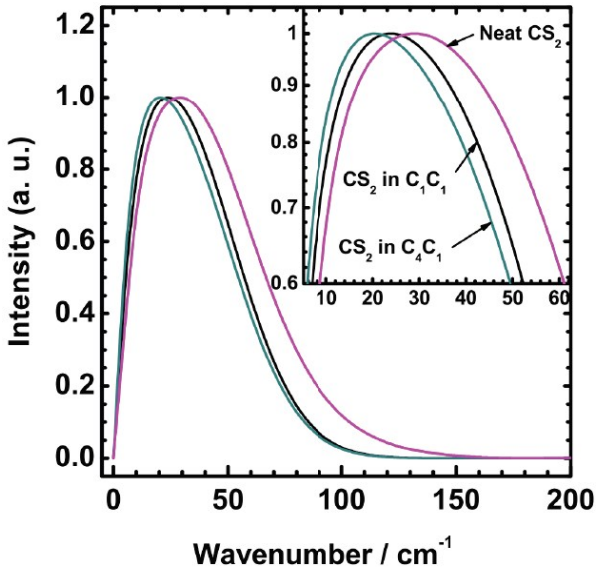

Fig. 8 Comparison of OHD-RIKES spectra of CS_2 in different environments. The height-normalized reduced spectral density of CS_2 from neat CS_2 and the CS_2 contributions to the reduced spectral densities of the 10 mol% mixtures of CS_2 in $[C_1C_1im][NTf_2]$ and $[C_4C_1im][NTf_2]$ are shown. Spectral parameters are given in Table 3. The inset shows an expanded view of the spectra in the region of the peak. Adapted from Figure 5 of Xue et al.[18]

.